Stability of the Ce_2O_3 phases: A DFT+U investigation

Juarez L. F. Da Silva*
Institut für Chemie, Humboldt-Universität zu Berlin, Unter den Linden 6, D-10099 Berlin, Germany
(Dated: October 24, 2007)

We report a first-principles investigation of the energetics and structure properties of $CeO_{1.50}$ in the hexagonal (La_2O_3), cubic (bixbyite), and monoclinic structures. Our calculations are based on density functional theory within the local density approximation (LDA), generalized gradient approximation (GGA), LDA+U, and GGA+U functionals. The hexagonal (cubic) structure is 53 meV/$CeO_{1.50}$ (57 meV/$CeO_{1.50}$) lower in energy than the cubic (hexagonal) structure using LDA+U (GGA+U), which is consistent (in disagreement) with experimental observations. Thus, these results might indicates a superior description of cerium oxides by the LDA+U functional. We found that $V_0^{\mathrm{CeO_{1.50},\ hexagonal}} \approx V_0^{\mathrm{CeO_2},\ \mathrm{fluorite}}$, while $V_0^{\mathrm{CeO_{1.50}},\ \mathrm{cubic}}$ is $4-9\%$ larger than $V_0^{\mathrm{CeO_2},\ \mathrm{fluorite}}$, where V_0 is the equilibrium volume per formula unit. We explained the volume expansion of $CeO_{1.50}$ (cubic) compared to the bulk CeO_2 as a consequence of the change in the oxidation state of the Ce atoms from Ce^{IV+} in CeO_2 to Ce^{III+} in $CeO_{1.50}$ and due to the high stability of partially reduced CeO_2 in the cubic-like structure.

PACS numbers: 71.15.Mb,71.15.Ap,71.20.Eh
Keywords: density functional theory,Hubbard approach, cerium oxides, Ce_2O_3, stability

Cerium oxides (CeO_{2-x}, $0 \leq x \leq \frac{1}{2}$) and related compounds such as $Ce_{1-x}Zr_xO_2$ play an important role in catalysis.[1] CeO_{2-x} is a key component in automotive three-way catalyts used to decrease pollutants from combustion exhaust.[2,3] Catalysts based on Pt-CeO_{2-x} and Au-CeO_{2-x} have been investigated for the water-gas-shift reaction[4,5] ($CO + H_2O \longrightarrow CO_2 + H_2$) and Rh-$CeO_{2-x}$ for the steam-reforming reaction[6] ($C_2H_5OH + H_2O \longrightarrow 2CO + 4H_2$), which are key steps in fuel processing technology to generate H_2. Furthermore, cerium oxides have been extensively investigated as a support for vanadium catalysts.[7]

The main role of cerium oxides in catalysis has been attributed to the ability to easily take up and release oxygen under oxidizing and reducing conditions, respectively, which is known as oxygen storage capacity (OSC).[1] Thus, the reduction of CeO_2 in the fluorite structure into $CeO_{1.50}$ in the hexagonal $LaO_{1.50}$ structure ($CeO_2 \longrightarrow CeO_{1.50} + \frac{1}{2}O_2$) plays an important role in OSC.[1,8] It has been reported that partially reduced CeO_2 is stable in the cubic structure up to $x \sim 0.40$, which can be reoxidized to CeO_2 by exposure to an oxidizing environment.[1] For example, $CeO_{1.66}$ and $CeO_{1.68}$ have a cubic superstructure with the lattice parameter twice as larger as for the fluorite CeO_2 structure.[9] Thus, the phase transformation of partially reduced CeO_{2-x} (cubic structure) into $CeO_{1.50}$ (hexagonal structure) occurs only for oxygen compositions close to 1.50. Therefore, it important to undertand the stability of the different phases of $CeO_{1.50}$, in particular, the stability of the hexagonal structure compared to the cubic phase of $CeO_{1.50}$.

The theoretical description of Ce-based compounds have been a challenge for theoretical calculations based on density functional theory (DFT) employing local or semilocal exchange-correlation (XC) functionals due to the localized and extended behavior of the Ce $4f$-states in Ce-based compounds.[10] Recent calculations employing DFT+U,[11–14] in which a Hubbard U term is added to the local density approximation (LDA) or generalized gradient approximation (GGA),[15] yielded the correct ground state solution (insulator) of cerium oxides, in particular for Ce_2O_3, which cannot be obtained by plain DFT calculations, e.g., DFT-LDA/GGA yields a metallic solution for Ce_2O_3.[11,13] Furthermore, LDA+U and GGA+U results are in excellent agreement with hybrid functional calculations,[13] in which a percentage of the exact Fock exchange is added to the XC functional. Thus, DFT+U yields a superior description of the cerium oxides properties than plain DFT, however, as for plain DFT calculations, DFT+U rely on the choose of a particular XC functional to which the Hubbard U is added, e.g., LDA+U or GGA+U, as well as on the value of the effective Hubbard U term.

In this work, we addressed the following problems employing DFT+U calculations: (*i*) Stability of $CeO_{1.50}$ in the hexagonal, cubic, and monoclinic structures. (*ii*) Volume expansion effect of CeO_{2-x} upon reduction conditions. (*iii*) Performance of the LDA+U and GGA+U functionals in the study of cerium oxides, in particular, the stability of the bulk $CeO_{1.50}$.

The spin-polarized calculations are based on DFT+U and employing the projected augmented wave (PAW) method[16–18] as implemented in the Vienna ab-initio simulation package (VASP).[19,20] In DFT+U a Hubbard U term corresponding to the mean-field approximation of the on-site Coulomb interaction is added to the LDA or GGA functionals. We employed the rotationally invariant approach,[15] in which the Coulomb, U, and exchange, J, parameters do not enter separately but only the difference is meaningful ($U_{\mathrm{eff}} = U - J$). An effective Hubbard parameter of 5.30 eV (LDA+U) and

4.50 eV (GGA+U) was added only for the Ce $4f$-states, which was used in previous first-principle calculations for cerium oxides.[13,21] For comparison, LDA and GGA calculations were also performed. The Ce $4f$-states were considered in the valence for all calculations. Furthermore, we performed also GGA calculations in which the Ce $4f$-states were considered as part of the core, which was previosly used in the study of the OSC in cerium oxides.[8] The frozen core states are treated fully relativistically, while the valence states are treated by the scalar relativistic approximation, i.e., spin-orbit coupling is not taken into for the valence states. A plane-wave cutoff energy of 400 and 800 eV were chosen for the total energy and stress tensor calculations, respectively. The Brillouin-zone integrations were performed using a **k**-mesh of (10×10×5), (4×4×4), and (4×4×3), for the hexagonal, cubic, and monoclinic structures, respectively. All forces are optimized up to be smaller than 0.01 eV/Å.

All the rare-earth sesquioxides, under a temperature of $\sim$ 2000 °C, crystallize in one or three crystal structures,[22,23] namely, hexagonal,[24] monoclinic,[25] and body-centered cubic (bcc) structure.[26] The hexagonal structure (A-type, space group $P\bar{3}2/m1$, No. 164) has 2 f.u. ($CeO_{1.50}$) per unit cell, in which there are two internal parameters (u_{Ce}, u_O) to be determined in addition to the two lattice parameters (a_0, c_0).[24] The monoclinic structure (B-type, space group $C2/m$) has 6 f.u. per unit cell. There are three and five non-equivalent Ce and O atoms, respectively.[25] The bcc structure (C-type, space group $Ia\bar{3}$, No. 206), which is also known as bixbyite structure, has 16 f.u. per unit cell.[26] There are four internal parameters and one lattice parameter to be determined, i.e., ($u_{Ce}, x_O, y_O, z_O, a_0$). There is a close relation between the bixbyite $CeO_{1.50}$ structure and the fluorite CeO_2 structure, i.e., the bixbyite structure can be derived by removing 25% of the oxygen atoms and then rearranging the remaning atoms somewhat. The structures are show in Fig. 1, while the results for the lattice parameters are summarized in Table I.

The cubic structure has the largest equilibrium volume per f.u., V_0, among the calculated structures, while the monoclinic structure has the smallerst one, i.e., ($V_0^{\text{monoclinic}} < V_0^{\text{hexagonal}} < V_0^{\text{cubic}}$). This trend was obtained by all XC functionals. For the hexagonal structure, LDA+U underestimates V_0 by 3.2%, while GGA+U overestimates by 3.3% compared with experimental results,[24] i.e., similar magnitudes, but opposite directions. For the cubic phase, there are experimental results only for $x = 1.53$ and 1.68.[9,23] For $x = 1.53$, which is the closest oxygen composition to $x = 1.50$, LDA+U yields almost the experimental equilibrium volume, i.e., a difference smaller than 0.2%, however, GGA+U overestimates V_0 by 4.6%. In contrast to the results obtained for the hexagonal phase, the LDA+U and GGA+U functionals yield unexpected small and large deviations for V_0^{cubic}, which might indicate a large uncertainty in the equilibrium lattice constants of $CeO_{1.50}$ in the cubic phase.

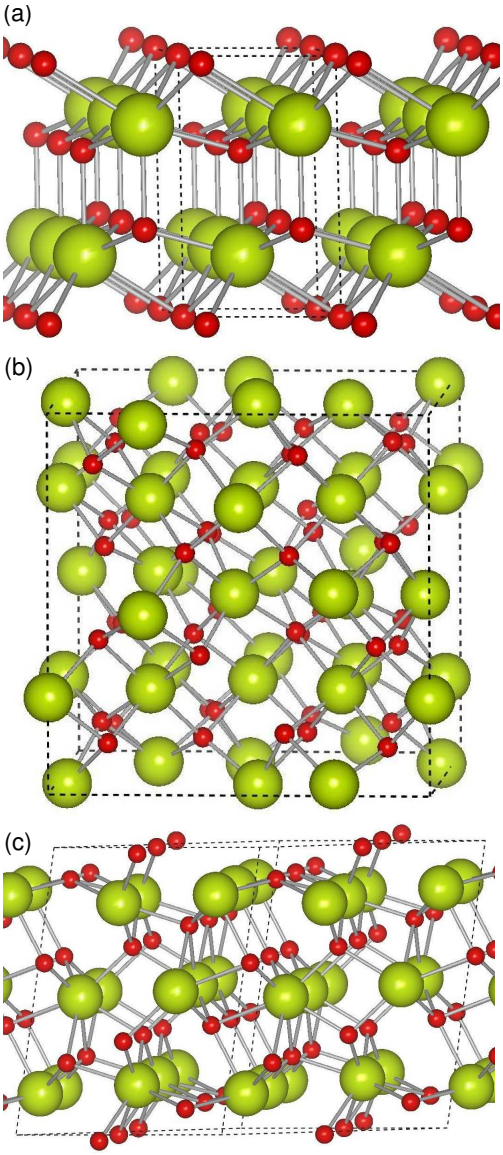

FIG. 1: (Color online) Bulk structures of $CeO_{1.50}$. (a) hexagonal La_2O_3 structure. (b) cubic bixbyite structure. (c) Monoclinic structure. The large and small balls indicate Ce and O atoms, respectively. The cells indicated by dashed lines are the primitive ones for the hexagonal and monoclinic structures and the conventional one for the cubic bixbyite structure.

From our knowledge, the monoclinic structure has not been experimentally observed for $CeO_{1.50}$.[23]

Experimental studies have obtained that the equilibrium volume of CeO_2 increases upon reduction of CeO_2 under H_2 atmosphere, e.g., $V_0^{CeO_2}$ increases up to $\sim$ 7% at partial reduction conditions.[27,28] Using the equilibrium volumes of CeO_2 in the fluorite structure per f.u. [39.36 (LDA+U), 41.37 (GGA+U), 38.71 (LDA), and 40.92 Å^3 (GGA)][13] and our results obtained in this work for the reduced $CeO_{1.50}$ in the cubic phase, we found that

TABLE I: Structural parameters of $CeO_{1.50}$ in the hexagonal, monoclinic, and cubic structures. Equilibrium volume, V_0, per formula unit, equilibrium lattice constants (a_0, b_0, c_0), internal parameters, and angle between the lattice vectors, β, for the monoclinic structure.

Hexagonal structure					
	V_0 (Å^3)	a_0 (Å)	c_0 (Å)	u_{Ce}	u_O
LDA+U^a	38.46	3.87	5.93	0.2441	0.6463
GGA+U^a	41.03	3.92	6.18	0.2471	0.6448
LDA^a	36.11	3.77	5.88	0.2429	0.6413
GGA^a	38.67	3.83	6.08	0.2459	0.6430
GGA^b	41.75	3.94	6.20	0.2485	0.6445
Exp.^{c}	39.72	3.89	6.06	0.2454	0.6471
Monoclinic structure					
	V_0 (Å^3)	a_0 (Å)	b_0 (Å)	c_0 (Å)	β
LDA+U^a	37.88	13.92	3.58	9.23	99.14
GGA+U^a	40.38	14.24	3.65	9.44	99.28
LDA^a	35.04	13.53	3.47	9.07	99.20
GGA^a	37.85	13.94	3.57	9.27	99.57
GGA^b	41.01	14.30	3.67	9.50	99.18
Cubic structure						
	V_0(Å^3)	a_0(Å)	u_{Ce}	x_O	y_O	z_O
LDA+U^a	43.39	11.16	0.4701	0.3893	0.1481	0.3782
GGA+U^a	45.45	11.33	0.4716	0.3887	0.1482	0.3792
LDA^a	40.35	10.89	0.4793	0.3860	0.1440	0.3773
GGA^a	42.99	11.12	0.4789	0.3874	0.1452	0.3775
GGA^b	46.54	11.42	0.4699	0.3904	0.1489	0.3783
Exp.^{d}	43.44	11.16				
Exp.^{e}	42.85	11.11				

[a]PAW calculations with the Ce $4f^1$-state in the valence.
[b]PAW calculations with the Ce $4f^1$-state in the core.
[c]Experimental results, Ref. 24.
[d]Ref. 23; result for $CeO_{1.53}$.
[e]Ref. 9; result for $CeO_{1.68}$.

$V_0^{CeO_{1.50},\ cubic}$ increases by $4-9\%$ compared to the equilibrium volume of CeO_2. Furthermore, we found that $V_0^{CeO_2} \approx V_0^{CeO_{1.50},\ hexagonal}$. Therefore, only the results obtained for $CeO_{1.50}$ in the cubic structure can explains the volume expansion of CeO_2 upon reduction conditions, which provides further evidences for a cubic-like structure for partially reduced CeO_2. We explains the lattice expansion effect of CeO_2 upon reduction conditions as a consequence of the changes in the oxidation state of the Ce atoms upon reduction conditions and to the high stability of the cubic-like structure of CeO_2 upon reduction conditions. For example, Ce atoms change the oxidation state from Ce^{IV+} in CeO_2 to Ce^{III+} in $CeO_{1.50}$, which implies a change in the size of the Ce atoms from 0.97 to 1.14 Å,[29,30] respectively, and hence, induces an expansion of the equilibrium volume. Therefore, we conclude that the high stability of the reduced CeO_2 phase (cubic-like structure) plays an importante role in the lattice expansion effect.

The relative total energies per f.u., ΔE_{tot}, with respect to the hexagonal structure are summarized in Table II. $\Delta E_{tot}^{structure} = E_{tot}^{structure} - E_{tot}^{hexagonal}$. We found that the monoclinic structure has the highest energy among the three studied structures, which was expected, i.e., there is no reported observation of the monoclinic structure for $CeO_{1.50}$. The LDA+U, GGA+U, and GGA ($4f$-state in the core) functionals obtained $\Delta E_{tot}^{monoclinic} \approx$ 125 meV, while the LDA and GGA functionals yielded about 50 meV. Thus, the localization of the Ce $4f$-states increases the stability of the hexagonal structure compared with the monoclinic phase.

TABLE II: Relative total energy, ΔE_{tot}, of $CeO_{1.5}$ given in meV per formula unit in the hexagonal, monoclinic, and bcc structures. $\Delta E_{tot}^{structure} = E_{tot}^{structure} - E_{tot}^{hexagonal}$.

	hexagonal	cubic	monoclinic
LDA+U^a	0.00	+53	+128
GGA+U^a	0.00	−57	+123
LDA^a	0.00	+31	+52
GGA^a	0.00	−111	+56
GGA^b	0.00	−105	+122

[a]Present study: Ce $4f$-states in the valence.
[b]Present study: Ce $4f$-states in the core.

The hexagonal structure has the lowest total energy among the three studied structures employing the LDA+U and LDA functionals, which is consistent with experimental observations.[24] However, in contrat with experimental results, the cubic structure has the lowest total energy using the GGA+U and GGA (Ce $4f$-states in the valence and in the core) functionals. To cross-check this particular discrepancy between the XC functionals, which may depend on the performance of the PAW potentials to describe Ce-based compounds, we performed calculations employing the all-electron full-potential linearized augmented plane-wave (FP-LAPW) method, as implemented in the WIEN2k package.[31] For the FP-LAPW calculations, the core states were treated fully relativistically, while the semi-core and valence states are treated by the scalar relativistic approximation. We found that $\Delta E_{tot}^{cubic} = -47$ (GGA+U), -96 (GGA), $+64$ (LDA+U), and 43 meV (LDA), which is consistent with the PAW results. Hence, these results are not an artifact from the PAW potentials. Hence, the present results might indicate that the LDA+U functional provide a superior description of the stability of the $CeO_{1.50}$ compounds compared with the GGA+U functional. For the FP-LAPW calculations, the optimized PAW LDA+U and GGA+U structures were used, while for LDA and GGA the structures were fully optimized using the FP-LAPW method. Atomic foces are not implemented in the WIEN2k package within the DFT+U framework.

As mentioned in the introduction, the reduction energy to reduce CeO_2 into $CeO_{1.50}$ ($CeO_2 \rightarrow CeO_{1.50} + \frac{1}{4}O_2$), is an important quantity, and it has been the subject of several recent studies.[12–14,32] We found that the relative total energy difference between the hexagonal and cubic structures is only few tenths of meV per f.u., hence, the choice of the $CeO_{1.50}$ structure does not play a critical role in the calculation of the reduction energy. This

finding is contrast to the relative reduction energy difference of 0.82 eV between cubic and hexagonal structures reported in Ref.[32]. This large difference is due to the approximation of the complex cubic bixbyite structure by the fluorite-like structure with 25% of oxygen vacancies, as reported in Ref.[32]. Therefore, conclusions based on that particular approximation should be taken with caution.

As metioned above, LDA+U yields a superior description of the stability of $CeO_{1.50}$, and hence, bulk modulus calculations were performed using only the LDA+U functional. The bulk modulus, B_0, for the different phases were obtained by fitting of the relaxed potential energy surface (13 regularly space volumes) to the Murnaghan's equation of state. We obtained 1.30, 1.53 and 1.24 Mbar for the hexagonal, cubic, and monoclinic structures, respectively, while $B_0 = 2.10$ Mbar for CeO_2 using LDA+U.[13] Thus, the formation of oxygen vacancies in the fluorite CeO_2 structure and changes in the oxidation state of the Ce atoms decreases the bulk modulus from 2.10 to 1.53 Mbar. Furthermore, B_0 decreases from 1.53 to 1.30 Mbar due to the phase transition from cubic to the hexagonal structure.

In summary, we reported DFT+U and DFT calculations for the $CeO_{1.50}$ system in the hexagonal, cubic, and monoclinic structures. We found that the LDA+U and LDA functionals yielded the lowest total energy for the hexagonal structure, which is consistent with experimental observations, however, GGA+U and GGA (Ce $4f$-states in the valence or in the core) calculations are in contrast with the experimental results. Therefore, our results might indicate that LDA+U provide a superior description of the cerium oxides than the GGA+U functional. Plain DFT calculations yield a metallic solution for $CeO_{1.50}$ however, the stability of $CeO_{1.50}$ and structure properties are consistent with DFT+U calculations. Furthermore, we explain the volume expansion effect of the CeO_2 upon reduction conditions as a consequence of the changes in the oxidation state of Ce atoms from Ce^{IV+} in CeO_2 to Ce^{III+} in $CeO_{1.50}$ and due to the high stability of the partially reduced CeO_2 in the cubic-like structure.

This work was supported by the Deutsche Forschungsgemeinschaft (Sonderforschungsbereich 546). The calculations were carried out on the IBM pSeries 690 system system of the Norddeutscher Verbund für Hoch- und Höchstleistungsrechnen (HLRN). I would like to thanks Joachim Sauer and M. Veronica Ganduglia-Pirovano for fruitful discussions.

* Present address: National Renewable Energy Laboratory, 1617 Cole Blvd., Golden, Colorado 80401, USA.; E-mail: juarez_dasilva@nrel.gov

[1] A. Trovarelli, Catal. Rev.-Sci. Eng. **38**, 439 (1996).
[2] A. Trovarelli, C. de Leitenburg, M. Boaro, and G. Dolcetti, Catal. Today **50**, 353 (1999).
[3] J. Kašpar, P. Fornasiero, and N. Hickey, Catal. Today **77**, 419 (2003).
[4] J. M. Zalc, V. Sokolovskii, and D. G. Löffler, J. Catal. **206**, 169 (2002).
[5] Q. Fu, H. Saltsburg, and M. Flytzani-Stephanopoulos, Science **301**, 935 (2003).
[6] G. A. Deluga, J. R. Salge, L. D. Schmidt, and X. E. Verykios, Science **303**, 993 (2004).
[7] I. E. Wachs, Catal. Today **100**, 79 (2005).
[8] N. V. Skorodumova, S. I. Simak, B. I. Lundqvist, I. A. Abrikosov, and B. Johansson, Phys. Rev. Lett. **89**, 166601 (2002).
[9] E. A. Kümmerle and G. Heger, J. Solid State Chem. **147**, 485 (1999).
[10] E. Wuilloud, B. Delley, W.-D. Schneider, and Y. Baer, Phys. Rev. Lett. **53**, 202 (1984).
[11] G. Kresse, P. Blaha, J. L. F. Da Silva, and M. V. Ganduglia-Pirovano, Phys. Rev. B **72**, 237101 (2005).
[12] D. A. Andersson, S. I. Simak, B. Johansson, I. A. Abrikosov, and N. V. Skorodumova, Phys. Rev. B **75**, 035109 (2007).
[13] J. L. F. Da Silva, M. V. Ganduglia-Pirovano, J. Sauer, V. Bayer, and G. Kresse, Phys. Rev. B **75**, 045121 (2007).
[14] C. Loschen, J. Carrasco, K. M. Neyman, and F. Illas, Phys. Rev. B **75**, 035115 (2007).
[15] S. L. Dudarev, G. A. Botton, S. Y. Savrasov, C. J. Humphreys, and A. P. Sutton, Phys. Rev. B **57**, 1505 (1998).
[16] P. E. Blöchl, Phys. Rev. B **50**, 17953 (1994).
[17] G. Kresse and D. Joubert, Phys. Rev. B **59**, 1758 (1999).
[18] O. Bengone, M. Alouani, P. Blöchl, and J. Hugel, Phys. Rev. B **62**, 16392 (2000).
[19] G. Kresse and J. Hafner, Phys. Rev. B **48**, 13115 (1993).
[20] G. Kresse and J. Furthmüller, Phys. Rev. B **54**, 11169 (1996).
[21] S. Fabris, S. de Gironcoli, S. Baroni, G. Vicario, and G. Balducci, Phys. Rev. B **72**, 237102 (2005).
[22] L. Eyring, *Handbook on the Pysics and Chemistry of Rare Earths* edited by K. A. Gschneider, Jr. and L. Erying (North-Holland Publishing Company, Amsterdam, 1979).
[23] G.-Y. Adachi and N. Imanaka, Chem. Rev. **98**, 1479 (1998).
[24] H. Bärnighausen and G. Schiller, J. Less-Common Met. **110**, 385 (1985).
[25] D. T. Cromer, J. Phys. Chem. **61**, 753 (1957).
[26] A. Bartos, K. P. Lieb, M. Uhrmacher, and D. Wiarda, Acta Cryst. B **49**, 165 (1993).
[27] V. Perrichon, A. Laachir, G. Bergeret, R. Fréty, L. Tournayan, and O. Touret, J. Chem. Soc. Faraday Trans. **90**, 773 (1994).
[28] C. Lamonier, G. Wrobel, and J. P. Bonnelle, J. Mater. Chem. **4**, 1927 (1994).
[29] R. D. Shannon and C. T. Prewitt, Acta Cryst. B **25**, 925 (1969).
[30] R. D. Shannon, Acta Cryst. A **32**, 751 (1976).
[31] P. Blaha, K. Schwarz, P. Sorantin, and S. B. Trickey, Comput. Phys. Commun. **59**, 399 (1990).
[32] L. Petit, A. Svane, Z. Szotek, and W. M. Temmerman,

Phys. Rev. B **72**, 205118 (2005).